In: AIAA SCITECH 2023 Forum 23-27 January 2023, National Harbor, Maryland, USA
DOI:10.2514/6.2023-0706

Mapping the Effect of Variable HPT Blade Cooling on Fuel Burn, Engine Life and Emissions for Fleet Optimization using Active Control

Evangelia Pontika[1], Panagiotis Laskaridis[2]
Cranfield University, Bedford, MK430AL, United Kingdom

Felipe Montana Gonzalez[3], Will Jacobs[4], Andrew Mills[5]
The University of Sheffield, Sheffield, S102TN, United Kingdom

Modern aero engines have increasingly sophisticated control systems. The aim for next-generation aircraft is to have even more adaptive and flexible control systems to enable the optimization of economic aspects, operational aspects and fleet management. Among others, an engine control variable that has the potential to offer various life and fuel burn benefits at different flight phases is the High-Pressure Turbine (HPT) blade cooling air. The HPT blades have demanding cooling requirements to protect their life and decelerate HPT efficiency degradation. However, any engine bleed has a penalty in efficiency and results in increased fuel consumption. Previous generation aircraft have a fixed relative blade cooling flow based on a design choice for a trade-off between life and efficiency. However, with adaptive control systems, there is an opportunity to extract the maximum potential benefit under different flight phases and scenarios. With this opportunity comes the challenge of increased complexity in engine behavior necessitating detailed modeling to quantify effects on lifing, fuel burn and safety. This paper focuses on modeling the performance, lifing and emission effects of variable HPT blade cooling air at take-off, climb and cruise. First, the effect of variable cooling on the Turbine Entry Temperature (TET), Exhaust Gas Temperature (EGT), fuel flow, lifing and NOx emissions are modeled at operating point level while the thrust requirement is achieved. Subsequently, a Design of Experiment is performed at mission level with the relative cooling flow at take-off, climb and cruise as the independent variables to train surrogate, analytical models. The analytical models are applied in the probabilistic modeling of system failure rates under different cooling flows. Optimization of engine control variables, in this case, the HPT blade cooling, requires analytical expressions that can be used in objective functions. These analytical models will inform fleet optimizers and active control systems to facilitate the implementation of fleet decisions such as reducing direct operating costs (fuel cost, maintenance reserves, NOx taxation), meeting NOx requirements of airports and extending Time-on-Wing (TOW). The findings indicate that take-off offers an opportunity to protect HPT life with increased cooling, but caution should be exercised in regard to the damage increase at the downstream non-cooled hot gas path components. A decrease in cooling flow at cruise, which is less detrimental to engine life, can offer significant fuel savings and climb

[1]Research Fellow in Propulsion Performance and Fleet Management, Centre for Propulsion and Thermal Power Engineering, AIAA member
[2] Professor of Hybrid Electric Propulsion, Centre for Propulsion and Thermal Power Engineering, AIAA member
[3] Research Fellow, Department of Automatic Control and Systems Engineering
[4] Research Fellow, Department of Automatic Control and Systems Engineering
[5] Senior Research Fellow, Department of Automatic Control and Systems Engineering

can be investigated for the optimum economic trade-off between life and fuel burn as a response to economic scenarios.

I. Nomenclature

C	=	material constant for creep
e_e	=	elastic strain
e_p	=	plastic strain
m	=	mass
m_c	=	cooling flow
N	=	shaft rotational speed
N_f	=	cycles to failure
r_{cg_sec}	=	distance of the center of gravity of the blade section from the rotation axis
stg	=	stage
T_{bc}	=	blade coolant side (cold side) temperature
T_{bg}	=	blade gas side (hot side) temperature
T_c	=	coolant temperature
T_g	=	gas temperature
t_r	=	creep rupture time
$T_{TBC,ext}$	=	thermal barrier coating external side temperature
$\Delta\varepsilon$	=	total strain range
$\Delta\varepsilon_e$	=	elastic strain range
$\Delta\varepsilon_p$	=	plastic strain range
ρ	=	density
σ_{CF}	=	centrifugal stress

II. Introduction

A. State of the Art

Modern gas turbines have increased flexibility and sophisticated control strategies to maximize efficiency, reduce fuel burn, protect engine life and ensure operating stability and safety. Apart from the fuel flow injection control system, some of the most well-documented control features of advanced gas turbines include the variable stator vane (VSV) angle [1,2] and handling bleed-offs to ensure compressor stability [3] at all power settings, the take-off derate to improve life consumption and climb thrust derate settings (with an option for slow and fast washout) to trade-off fuel burn and engine life [4,5]. In the most recent engines, active tip clearance control [6,7] is also used to improve engine efficiency by minimizing the gap between the tip and the casing while avoiding blade rubs under the variable disk and blade thermal and mechanical expansion over the mission.

B. Cooling Design

Gas turbines have been continuously evolving over the past decades to improve thermal efficiencies by increasing the Turbine Entry Temperatures (TET). To allow this gas temperature increase, advanced materials, thermal barrier coating and sophisticated cooling techniques have been developed. In modern engines, the TET can be as high as 1800-1900K [8], while the melting range of typical nickel superalloys is around 1500-1600K [9,10]. The cooling flow requirements of modern gas turbines with high operating temperatures can be as high as 20-30% [11,12]. However, any bleed has an efficiency penalty. In the case of High-Pressure Turbine (HPT) blade cooling, the efficiency loss comes through two main effects: 1. less airflow passes through the combustor to raise its enthalpy and produce work, and 2. the mixing of the cooling air with the main flow causes pressure losses [13]. Horlock et al. [13] observed that the potential gain in thermal efficiency from increasing the TET becomes marginal at very high temperatures because of the pressure losses imposed by the large cooling requirements and the downstream mixing of the cooling air. They also calculated the optimum pressure ratio to maximize thermal efficiency with a given TET and cooling flow. Lallini et al. [14] calculated the optimum cooling air schedule across a flight mission in terms of Specific Fuel Consumption (SFC) and compared it against constant cooling. They observed a 0.3 [mg/kN/s] improvement in cruise SFC with the optimum cooling air schedule. Torbidoni et al.[15] proposed an analytical model for the performance of the blade film cooling and mapped the effect of coolant mass flow and gas temperature on the blade temperature without addressing the effect on engine efficiency, fuel burn or lifing.

C. Motivation

The potential benefits of variable HPT blade cooling flow under different flight segments and economic scenarios have not been explored sufficiently in literature or implemented in commercial engines based on public information. However, it should be noted that a lot of recent developments in gas turbines are not available in the public domain due to the commercial sensitivity for manufacturers. Any bleed air extracted from the main airflow has an efficiency penalty and will require an increase in fuel burn and TET. Cooling systems of existing engines were designed based on trade-offs for efficiency penalty and engine degradation while taking into account material properties and tip clearances due to blade thermal expansion. However, the selection of a fixed cooling is highly influenced by the most demanding conditions at take-off, but at cruise, there might be an excess of cooling flow in terms of lifing, whereas the efficiency penalty becomes more important due to the long time that the engine spends at cruise, especially at medium- and long-range aircraft applications. This paper models the effect of variable cooling flow at mission level with a holistic approach that takes into account engine performance (fuel burn, TET, EGT, thrust requirement), emissions and lifing trade-offs between hot gas path components. Finally, analytical expressions that describe fuel burn, emissions and component severity as a function of cooling flows are extracted based on physics-based modeling. The analytical expressions can offer solutions to various economic scenarios such as an increase in fuel price or a requirement to extend Time-On-Wing (TOW), reduce maintenance reserves and meet airport NOx requirements, and can serve as objective functions for fleet optimization. Apart from reducing maintenance reserves, extending TOW can delay engine removals for scheduled shop visits during peak travel season or when there is an unavailability of spare engines or a specific part which may cause prolonged aircraft grounding

III. Methodology

D. Engine Performance and Flight Mission Analysis

The engine modeling with variable cooling and fixed target thrust is performed in Turbomatch [16], the in-house gas turbine performance simulation tool, in the Centre for Propulsion and Thermal Power Engineering Centre, at Cranfield University. The aircraft performance and flight path analysis is performed in Hermes [17], the in-house aircraft performance tool, which is coupled with Turbomatch to obtain the engine performance at each flight mission step.

In the present paper, a generic three-spool turbofan engine model and a typical long-range wide-body aircraft model are considered for the analysis. A combination of publicly available data and assumptions for the missing details is used. Some of the main characteristics are included in the Appendix.

E. Methodology for performance and lifing analysis

The flight mission analysis has as inputs the mission specifications (payload, range, cruise altitude etc), the engine and aircraft performance models, the thrust setting and the relative HPT blade cooling flow at take-off, climb and cruise. The outputs of the flight mission analysis provide aircraft performance indicators such as fuel burn, climb time, Rate of Climb (RoC) and engine performance parameters, including spool speeds, component gas temperatures, cooling flow, coolant temperature and air mass flow. For the examined components, the spool speed is input to the centrifugal stress calculation at each blade section, taking into account the span and the material of the blade. The gas temperature of each component is applied to a typical temperature distribution profile [18] because CFD analysis was out of the scope of this study and it would increase significantly the computational time for the multiple cooling flow combinations, phases and operating points that are analyzed over the mission. This research aims to capture generic sensitivities of engine performance, emissions and lifing to variable cooling based on a simplified, generic representation of the blade.

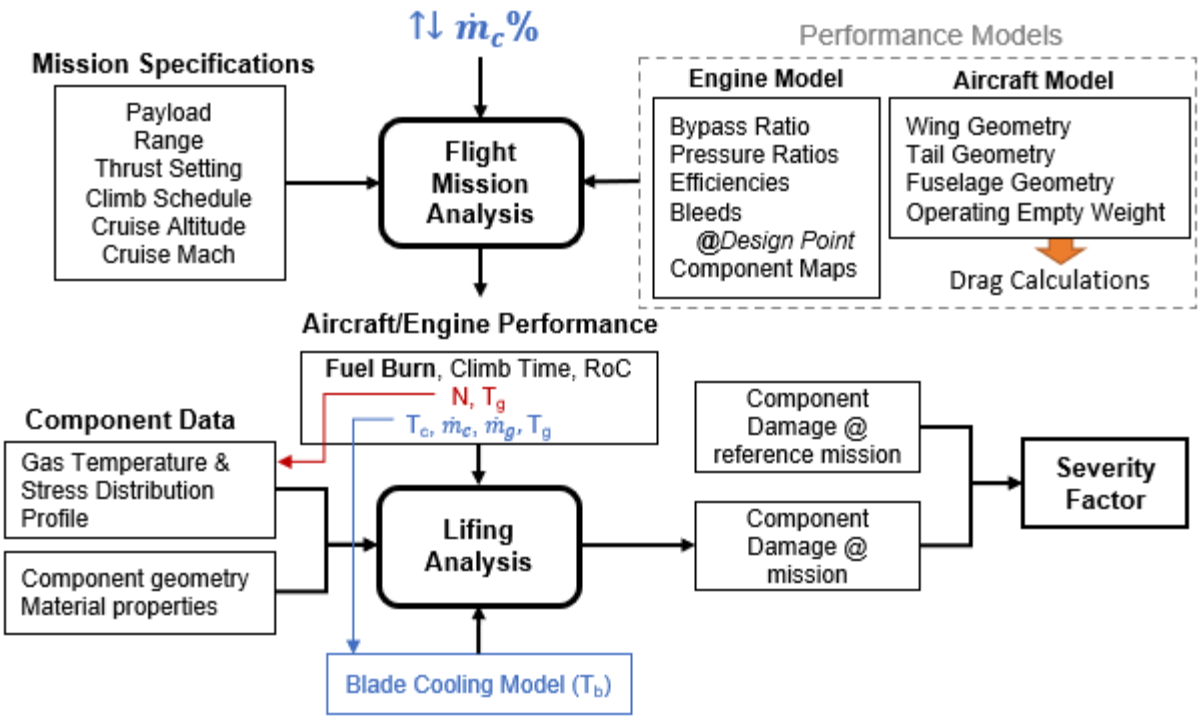

Fig. 1 Flight mission & lifing analysis overall methodology

The blade span, the thermal barrier coating (TBC) thickness, the blade thickness and material conductivities are input to the blade cooling model along with the cooling flow, gas flow, coolant temperature and gas temperature from the flight mission analysis. Therefore, a blade temperature distribution along the span at the leading edge is obtained. Finally, the blade temperature distribution profile and the stress distribution profile are input to the lifing analysis, which will be further analyzed in Section G. The damage fractions resulting from each mission are divided by the damage fraction of the mission with reference cooling flows to extract a severity factor.

F. Blade Cooling Model

The blade temperature for variable cooling is calculated using the analytical model presented by Eshati et al. [19]. The input parameters to the analytical heat transfer model for blade temperature are included in the Appendix. The blade is divided into uniform sections in the spanwise directions, similar to the section used for the stress calculation, so each section includes an element for the heat transfer calculation from the gas to the coolant as in Fig. 2. The coolant outlet temperature of each section becomes the coolant inlet temperature for the following section from root to tip.

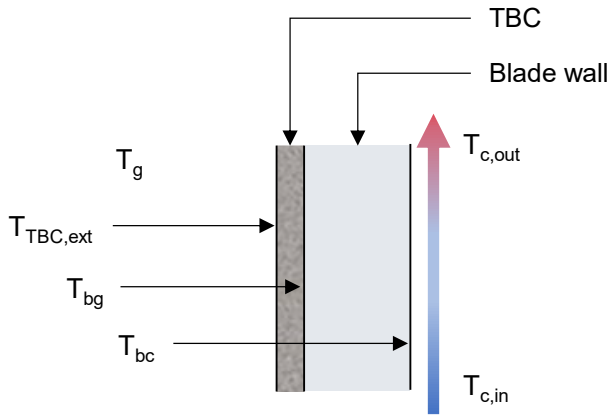

Fig. 2 Blade cooling model and temperature at the heat transfer areas

G. Lifing Analysis

1. Creep

The life analysis is based on creep, Low Cycle Fatigue (LCF) and oxidation damage. Creep is calculated using the Larson-Miller Parameter (LMP) [20].

$$LMP = T\frac{\log t_r + C}{1000} \tag{1}$$

Where tr is the time until rupture under the specified LMP and temperature, T is the temperature and C is a material constant which is usually set to 20 for nickel superalloys. The LMP under variable stress for CSM4-X, a representative nickel superalloy for gas turbine engines, is provided by Schneider [20] and it is fitted with a polynomial. During the flight mission analysis, the centrifugal stress is calculated at each blade section as a function of the rotational speed:

$$\sigma_{CF} = \frac{m_{sec} \cdot r_{cg\_sec} \cdot \omega^2}{A_{sec}} = \frac{m_{sec} \cdot r_{cg\_sec} \cdot 4\pi^2 \cdot N^2}{A_{sec}} = \rho_{material} \cdot h_{sec} \cdot r_{cg\_sec} \cdot 4\pi^2 \cdot N^2 \tag{2}$$

The blade geometry is simplified by considering the stresses and temperatures in the span direction at the leading edge, where the temperatures are the highest.

2. Low Cycle Fatigue

The low cycle fatigue is calculated using the Basquin/Coffin-Manson model, a strain-based method [21]:

$$\frac{\Delta\varepsilon}{2} = \varepsilon_\alpha = \frac{\Delta\varepsilon_e}{2} + \frac{\Delta\varepsilon_p}{2} = \frac{\sigma_f'}{E}\left(2N_f\right)^b + \varepsilon_f'\left(2N_f\right)^c \tag{3}$$

Nf represents the cycles until failure under the given loading conditions, $\Delta\varepsilon$ is the total strain range of the fatigue cycle, $\Delta\varepsilon_e$ is the elastic strain range and $\Delta\varepsilon_p$ is the plastic strain range. The fatigue cycles are extracted using the Rainflow method.

The elastic strain is calculated using Hooke's law [21]:

$$\varepsilon_e = \frac{\sigma}{E} \tag{4}$$

The plastic strain is calculated with the Ramberg-Osgood relationship [21]:

$$\varepsilon_p = \left(\frac{\sigma}{K}\right)^{\frac{1}{n}} \tag{5}$$

Where K is the strength coefficient (or the stress intercept at ε_p=1 in the stress-strain diagram)

3. Oxidation

The oxide thickness evolution is modeled using an Arrhenius-type equation provided by Meier et al [22]:

$$\delta = \left\{\exp\left[Q\left(\frac{1}{T_0} - \frac{1}{T}\right)\right] t\right\}^n \tag{6}$$

where δ is the oxide thickness, Q is the activation energy, T_0 is a temperature constant, T is the temperature and t is the exposure time. The constants are provided in [22].

A reference mission must be defined for the severity factor calculation. The severity factor is defined as the ratio between the damage fraction (or fraction of consumed life) of the current mission and the damage fraction of a reference mission [23].

$$\mathrm{SF} = \frac{damage\ fraction\ @\ given\ mission}{damage\ fraction\ @\ reference\ mission} \tag{7}$$

In the present context, the mission performed with the reference settings i.e. HPT blade cooling flow is treated as the reference mission.

H. Emissions Analysis

The NOx emissions are calculated using the P3-T3 method [24] and reference emission indices from the ICAO Aircraft Engine Emissions Databank [25] for a turbofan engine of similar class with the engine model used in this study.

I. Surrogate Modelling

The life analysis requires knowledge of the whole mission to extract fatigue cycles. Similarly, total fuel burn and total NOx are based on the whole mission, which is calculated using an iterative process until all the mission parameters converge. This complex process is not practical for fleet optimization and active control strategies. Simple analytical expressions are required in objective functions for optimization. For this reason, a surrogate model consisting of analytical expressions to capture the effect of variable cooling is developed.

A 5-level full factorial design is considered to create combinations of variable cooling flow at take-off, climb and cruise. This factorial design results in 216 datasets with unique combinations of cooling flow at take-off, climb and cruise. The output data are obtained using the framework in Fig. 1 with the cooling combinations of the factorial design as input settings. The range of the cooling is considered within the range of 4%-16% relative to high-pressure compressor (HPC) airflow. Descent is a less demanding phase with a very low thrust setting and the fuel burn, as well as life consumption at this phase, are of secondary importance compared to take-off, climb and cruise. However, potential benefits that can be harvested at descent with variable cooling flow may be investigated in future work.

Using the input and output datasets of the full factorial design, each output parameter is then fitted to an analytical equation with the relative cooling flow at take-off, climb and cruise as the independent input variables, using JMP software [26]. The produced surrogate model consisting of a set of analytical expressions can be described as:

$$\left(m_{fuel}, NOx, SF_{HPT}, SF_{IPT}, SF_{LPTstg1}\right) = f\left(\dot{m}_{c,rel,TO}, \dot{m}_{c,rel,Climb}, \dot{m}_{c,rel,cruise}\right) \tag{8}$$

IV. Findings

A. Constant Thrust with Variable Cooling

The TET, EGT, spool speed and fuel flow are modeled at take-off (Fig. 3). and Top of Climb (Fig. 4) when the relative cooling flow to the HPT blade is varied and the target thrust is fixed. At take-off, between 3% and 16% cooling flow, the TET has an increase of 120K to maintain the same thrust and the EGT an increase of 45K. Between the same two extremes, the fuel consumption increases from 3.71 kg/s to 3.83 kg/s.

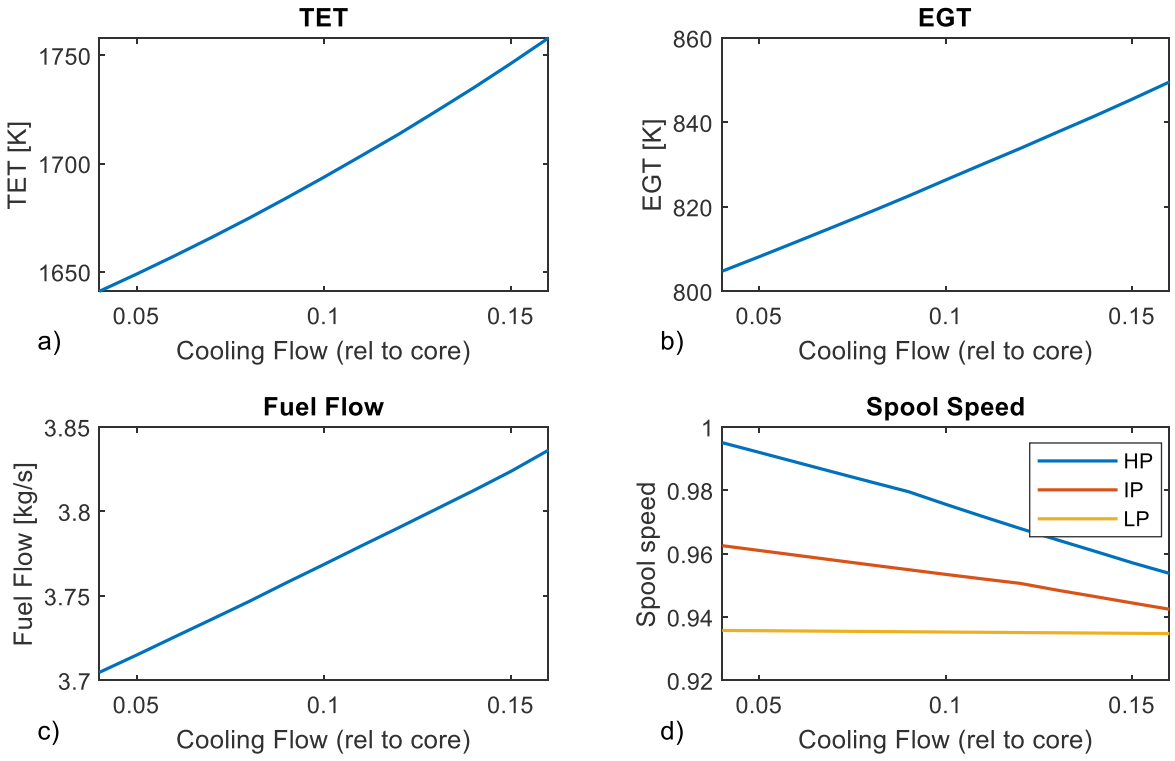

Fig. 3 TET, EGT, fuel consumption and spool speed over relative HPT cooling flow at take-off

In Fig. 4a, the absolute cooling flow that is fed to the HPT blades is plotted. Creep (Fig. 4b) and oxidation (Fig. 4c) life, along with centrifugal stress are expressed relatively with reference to 10% relative cooling flow. The centrifugal stress is related to fatigue life, however, since this is a sensitivity analysis at single operating point level, fatigue analysis cannot be performed because it requires a stress profile to extract the fatigue cycles. While HPT blade life is improved due to the increase in the cooling flow that reduces blade temperature, fuel flow and hence TET must increase to maintain the same thrust output, consequently, the downstream temperatures increase as well. However, the downstream components, the Intermediate-Pressure Turbine (IPT) and Low-Pressure Turbine (LPT), are not cooled so there is an increase in the effect of temperature-dependent mechanisms i.e., creep and oxidation. On the other side, the shaft speeds slightly decrease with increased cooling, with the HP spool having the most variation, consequently, low cycle fatigue damage is expected to reduce. For low cycle fatigue calculations, a stress profile is required to extract the fatigue cycles, however, in most cases, the major fatigue cycle of the mission is considered among engine start-up - maximum stress at take-off and engine shut-down. The fatigue effect is included in the mission level analysis further below in Fig. 14.

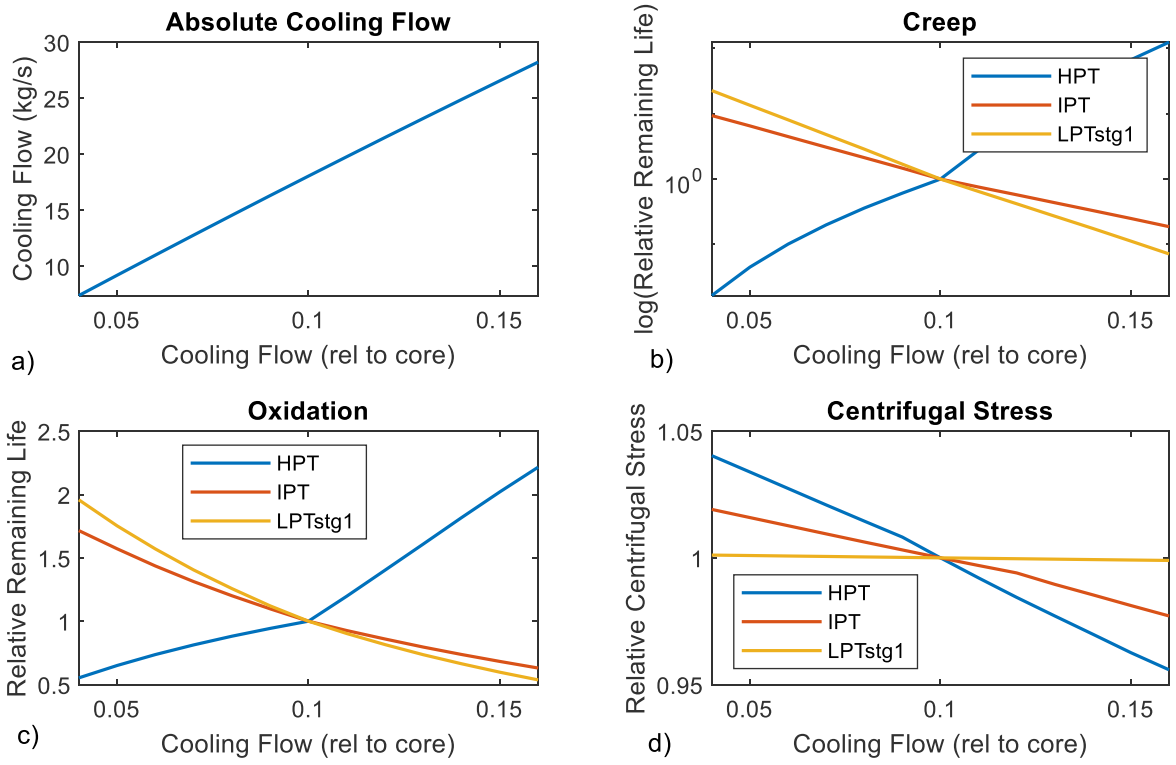

Fig. 4 Absolute cooling flow, relative creep life, relative oxidation life and relative centrifugal stress at HPT blade over variable relative HPT blade cooling flow at take-off

When the cooling flow increases, due to the air extraction from the HPC, the corrected air mass flow at the HPT reduces, consequently the relative HP spool speed reduces. This reflects on the HPC performance as well, which is coupled on the same shafts, so for higher cooling, the relative speed, the corrected mass flow and the pressure ratio reduce (Fig. 5).

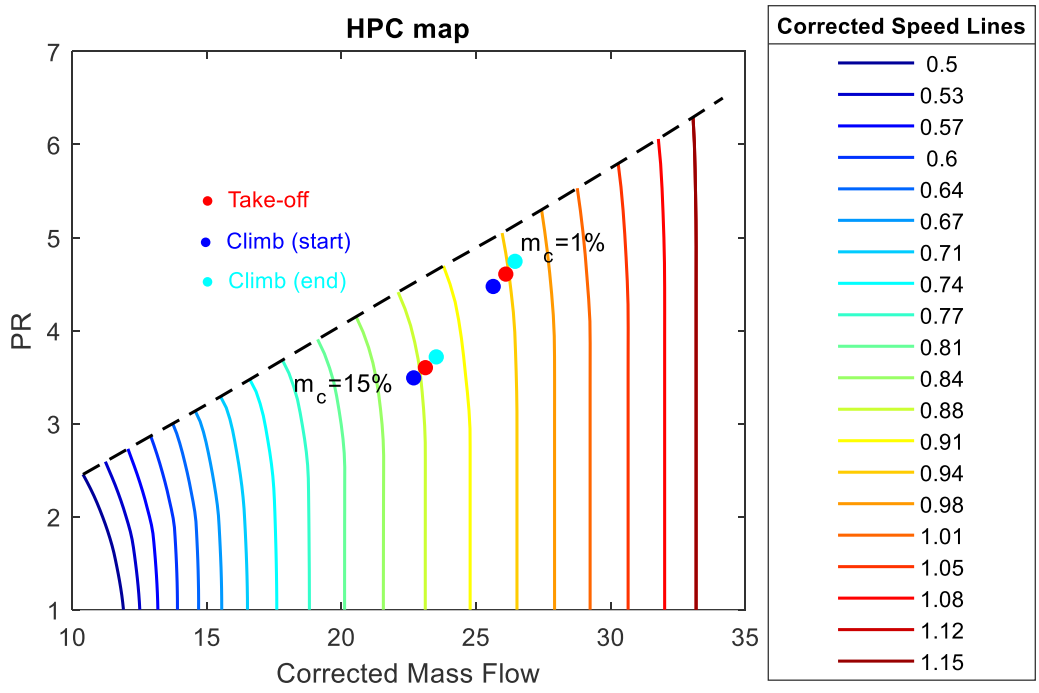

Fig. 5 Effect of variable cooling on HPC map operating points

The change in the compressor operating point, due to the variable bleed, has an impact on the NOx emission index, which is a function of P3, T3, FAR and fuel flow. When the cooling increases, the effect of lower combustor inlet pressure (P3) and temperature (T3) overcompensates for the increase in the fuel flow, so both the EINOx and NOx decrease (Fig. 6). The P3-T3 method is used in this study to provide a first indication about the effects on NOx emissions, however, further research may be required to verify the effect of variable cooling flow on NOx using higher fidelity methods than correlation-based methods.

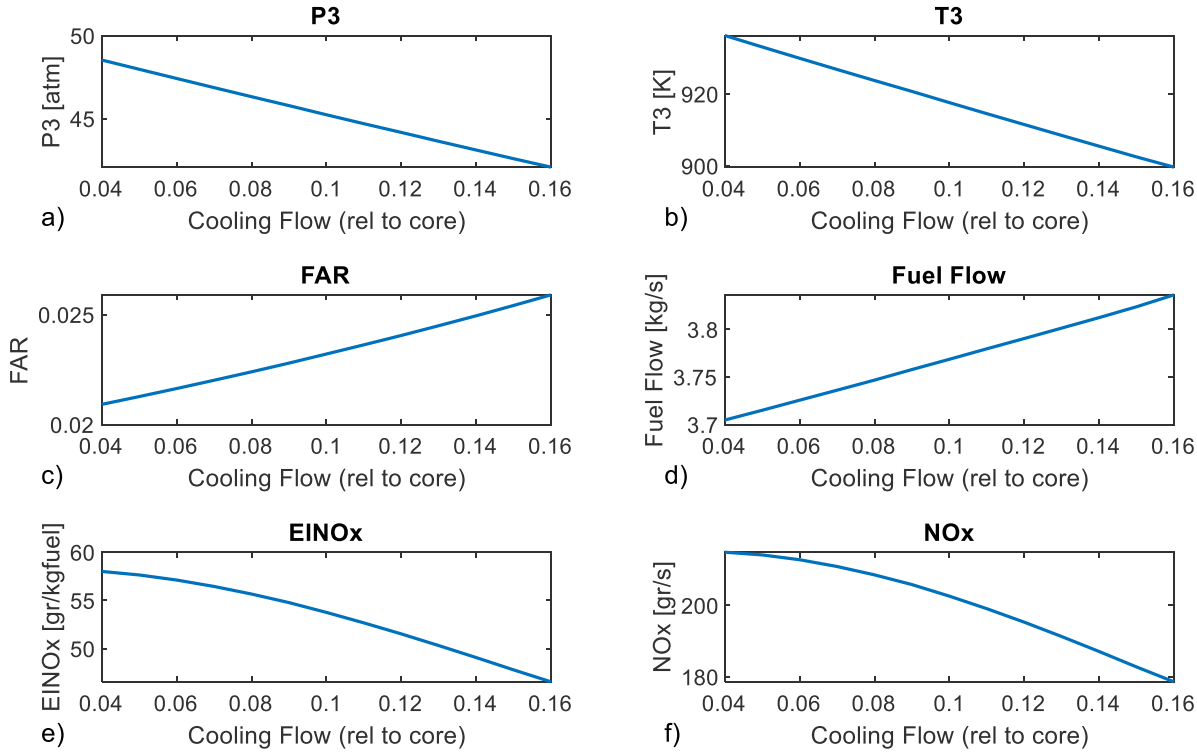

Fig. 6 Effect of relative cooling flow on NOx at take-off

Similar trends are observed at the ToC when variable cooling is applied. At ToC (Fig. 7), between 3% and 16% cooling flow, the TET (Fig. 7a) shows an increase of nearly 100K to maintain the same thrust and the EGT (Fig. 7b) an increase of 40K. Between the two extreme cooling flows, the fuel consumption increases from 1.635 kg/s to 1.678 kg/s. As also observed for take-off, the high-pressure (HP) spool speed has the maximum reduction in rotational speed among the three spools, from 95.9% to 92% when increasing the cooling flow from 3% to 16%.

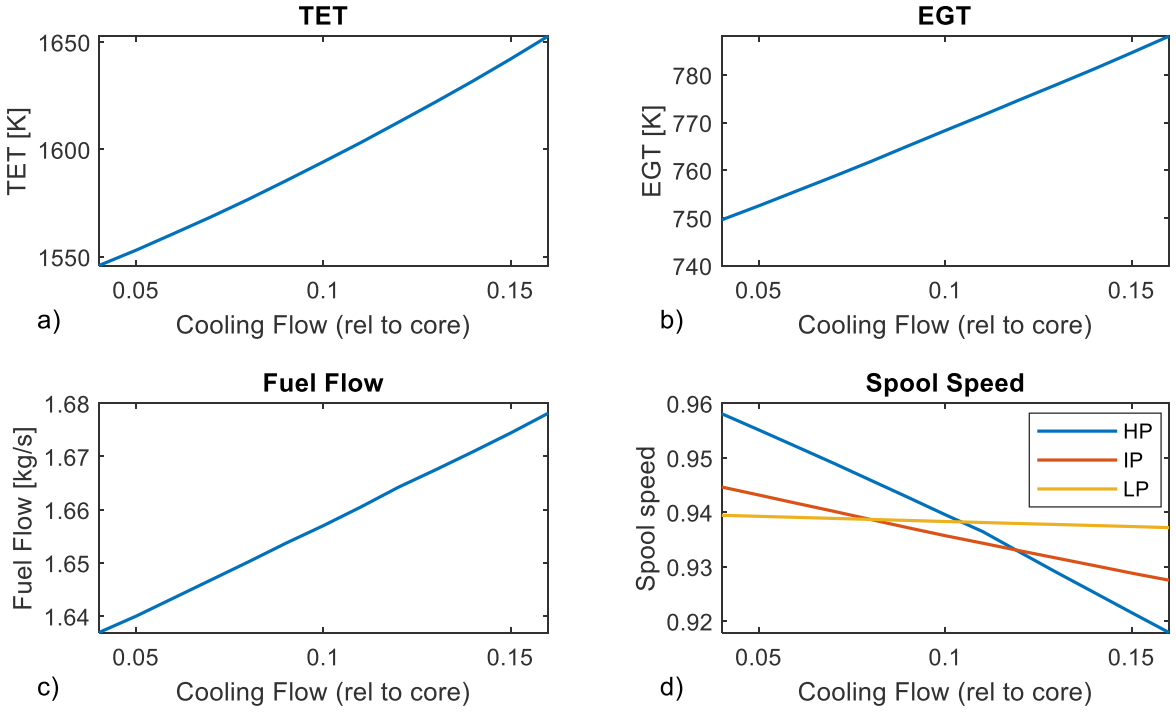

Fig. 7 TET, EGT, fuel consumption and spool speed over relative HPT cooling flow at ToC

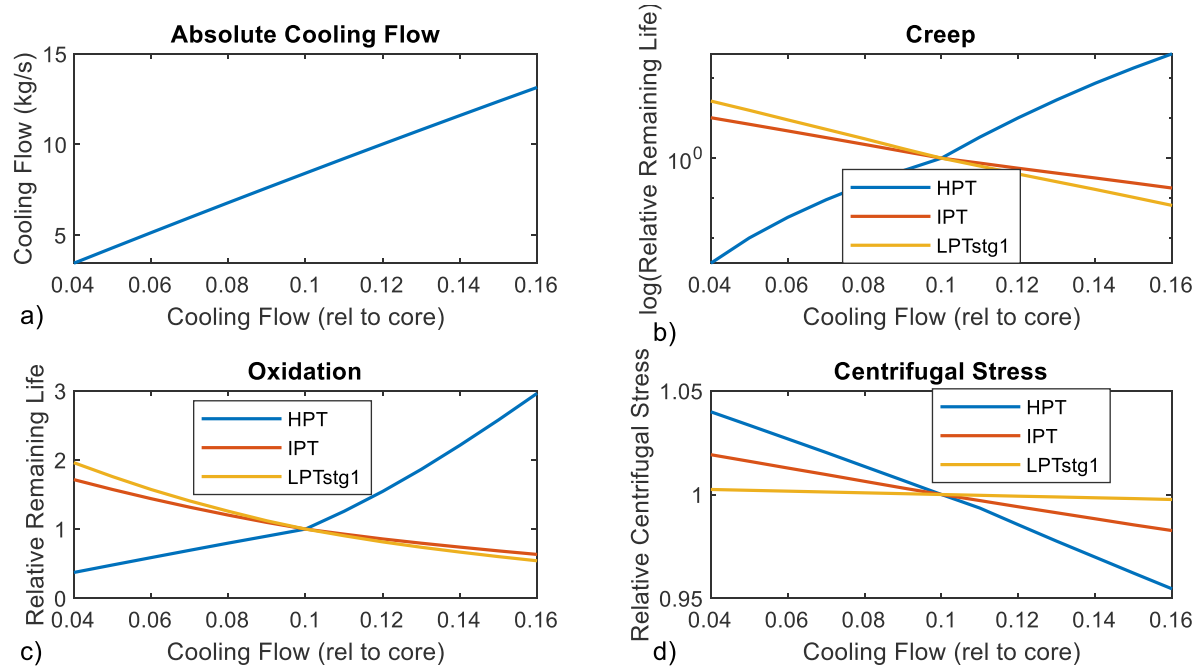

Fig. 8 Absolute cooling flow, relative creep life, relative oxidation life and relative centrifugal stress at HPT blade over variable relative HPT blade cooling flow at ToC

B. Life Analysis with Variable Cooling

Before proceeding to model multiple combinations of cooling flow in the full factorial design which increases the complexity and the number of cases, a sensitivity analysis is performed using the same cooling flow percentage (relative to HPC flow) across take-off, climb and cruise in order to understand the sensitivities and how the cooling flow selection effect propagates up to the final severity output. The flight profile (Fig. 9a) and the thrust profile (Fig. 9b) are maintained constant in all cases, but they are achieved with a different combination of cooling bleed, fuel flow and TET. The absolute cooling flow value over the flight time is presented in Fig. 9c and has a dramatic effect on the cooling effectiveness (Fig. 9d). For the extremely low 1% cooling flow the cooling effectiveness drops to 45% and for the highest value 15%, the cooling effectiveness reaches up to 83%.

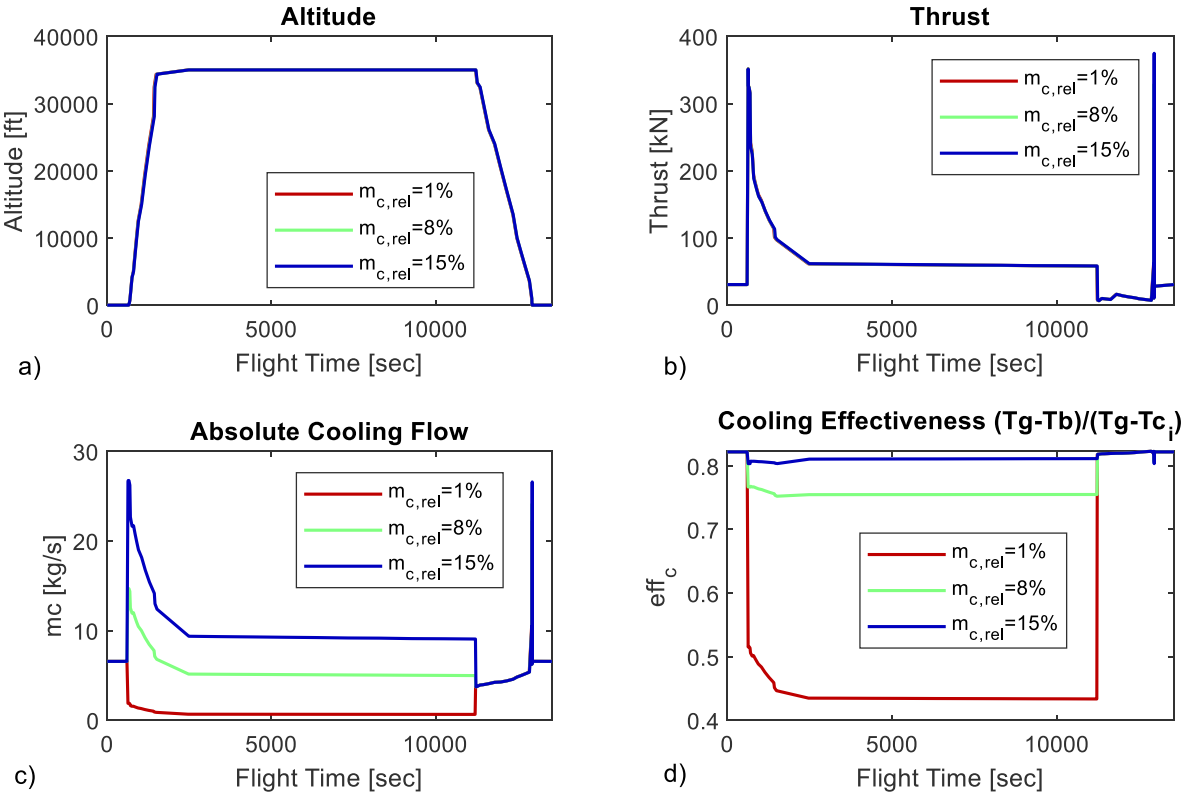

Fig. 9 Flight profile, thrust, cooling flow and cooling effectiveness over light time

To demonstrate how the variation of cooling flow is translated into different spanwise temperate distribution, coolant heating, blade temperature and centrifugal stress, which explains the change in the HPT blade severity factor, the results of two extreme cooling flows (1% and 15%) are presented. It would be a rather unrealistic design choice to have 1% HPT blade cooling flow at engines of this technology level with high TETs, but for the sake of demonstrating the sensitivities, two extreme cases are presented and discussed.

The cooling flow through the cooling channels of the HPT blade acts as a heat dump for the heat that is transferred from the hot gas to the blade. When the coolant flow is higher, the coolant needs more heat to be added to raise its temperature to the same temperature. Consequently, for higher cooling flow the coolant temperature will be increased more slowly along the blade span (Fig. 11b), maintaining its capability to remove heat more effectively from the blade due to the higher temperature difference between the coolant and the blade. In the extreme case of 1% cooling flow, at take-off, the coolant is heated from 1000K to 1500K between the root and the tip (Fig. 10b) while for 15% cooling the coolant is heated from 900K to 1050K at take-off (Fig. 11b).

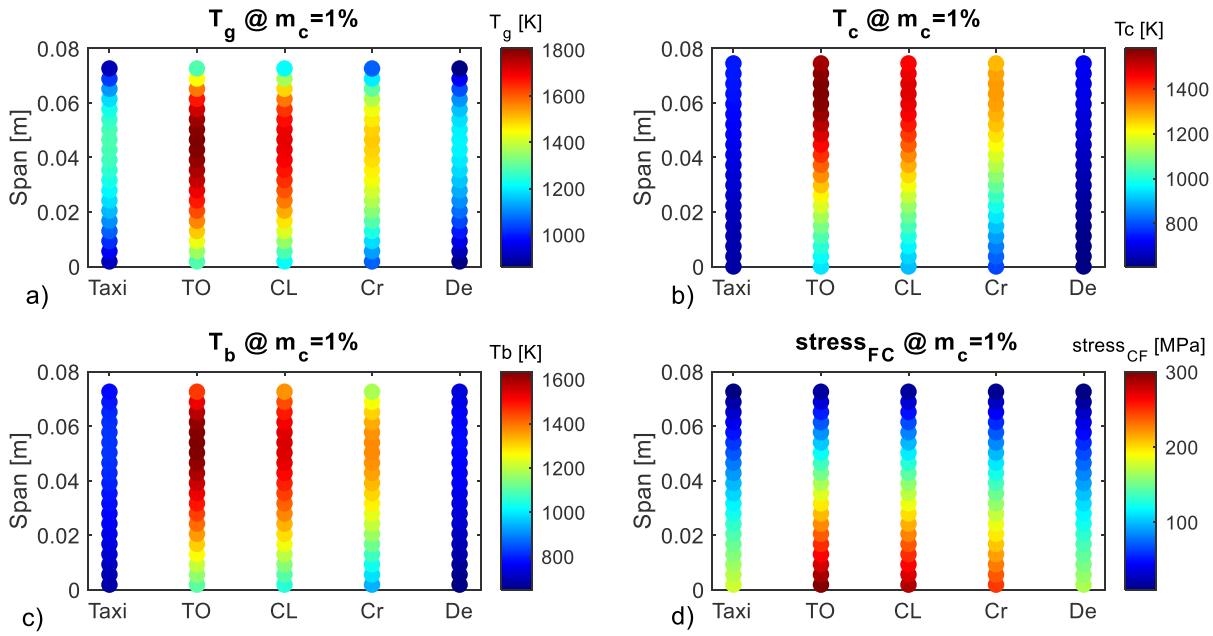

Fig. 10 Gas temperature, coolant temperature, blade temperature and centrifugal stress across the span at the leading edge of the HPT blade @ m_c=1%

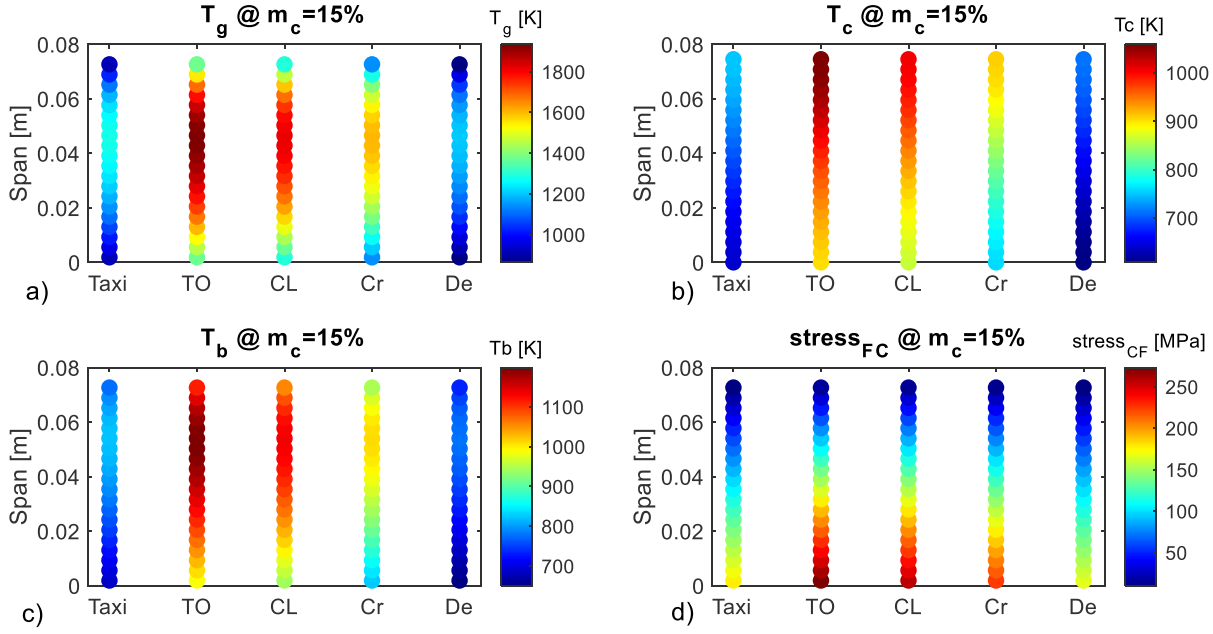

Fig. 11 Gas temperature, coolant temperature, blade temperature and centrifugal stress across the span at the leading edge of the HPT blade @ m_c=15%

By adding the ratio of time spent at each mission time step over the time until failure under the given conditions of the step, the consumed life (or damage fraction) due to each mechanism is calculated at the end of the mission. The two extreme cases of 1% and 15% cooling are presented in Fig. 12 and Fig. 13 respectively. Creep is very sensitive to temperature, so the relative creep factor is 10^{10} higher for 1% cooling flow compared to 15% cooling flow. The highest oxidation and creep damage appear at the blade span location with the highest temperature (Fig. 10c and Fig. 11c), while LCF damage is higher at the tip of the blade, where the centrifugal stress is the highest (Fig. 10d and Fig. 11d)

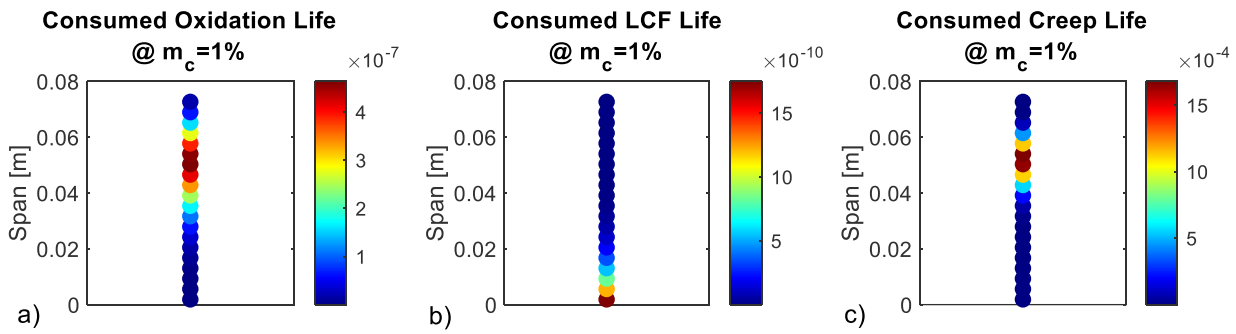

Fig. 12 Consumed life at the end of the mission @ m_c=1%

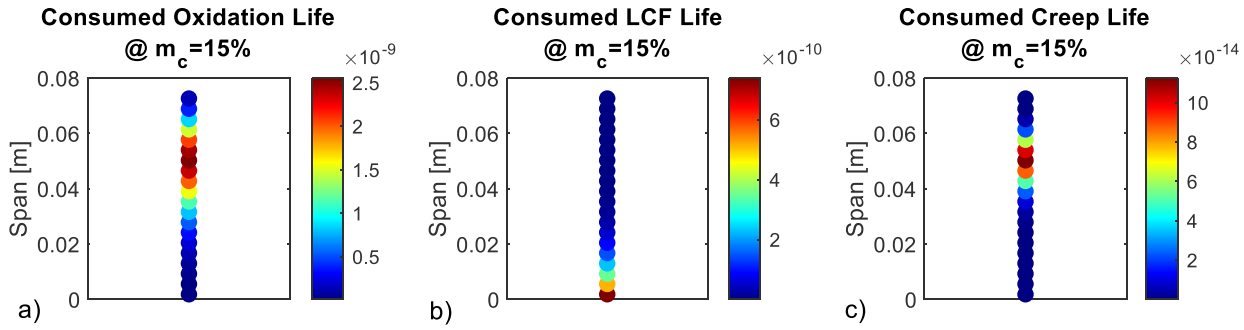

Fig. 13 Consumed life at the end of the mission @ m_c =15%

C. Design of Experiment

A surrogate model, consisting of analytical expression, has been created for a 3-hour mission with variable cooling at take-off, climb and cruise. The main output parameters of interest were fitted with analytical expressions, but with the same methodology, any other performance or lifing parameter of interest can be modeled. As described in Eq.(8), the inputs are the cooling flow (relative to the compressor flow) at take-off, climb and cruise and the outputs are the total mission fuel burn per engine, NOx emissions, and the severity factors of the HPT blade, IPT blade and LPT stg1 blade (Fig. 14). The CO_2 emissions can be simply considered directly proportional to the fuel burn ($3.16 kg_{CO2}/kg_{fuel}$ [27]) so there was no need for a surrogate. A multi-dimensional view of the surrogate model is presented in Fig. 14 to map the effects and some observations are discussed:

1. Trade-off between life and fuel burn

Increasing the cooling flow at take-off has a major impact on component severities, considering its short duration, while the total fuel penalty is small. Cruise cooling flow has the most significant effect on fuel burn (Fig. 14), hence CO_2 as well, due to the long cruise duration for long-range aircraft, while the effect on severity is lower than take-off and climb. Climb conditions, in terms of temperatures and duration, are in-between take-off and cruise, so climb has a more balanced trade-off between severity and fuel burn.

2. NOx effect

As explained earlier in Fig. 5, increasing the cooling reduces the compressor PR resulting in lower combustor inlet pressure, which reduces the NOx. Due to the much longer duration of cruise, the effect of take-off cooling on total mission NOx is small, but the isolated effect on airport NOx becomes more significant.

3. Component severity trade-off

Increasing the relative cooling flow to the HPT blade decreases the severity of the HPT blade. However, increasing the bleeds reduces the efficiency of the engine, so a higher TET is required to achieve the same target thrust. In the considered engine, the IPT and LPT are non-cooled, so these two components are directly exposed to the higher gas temperature and their severity increases (Fig. 14) when higher HPT cooling bleeds are extracted.

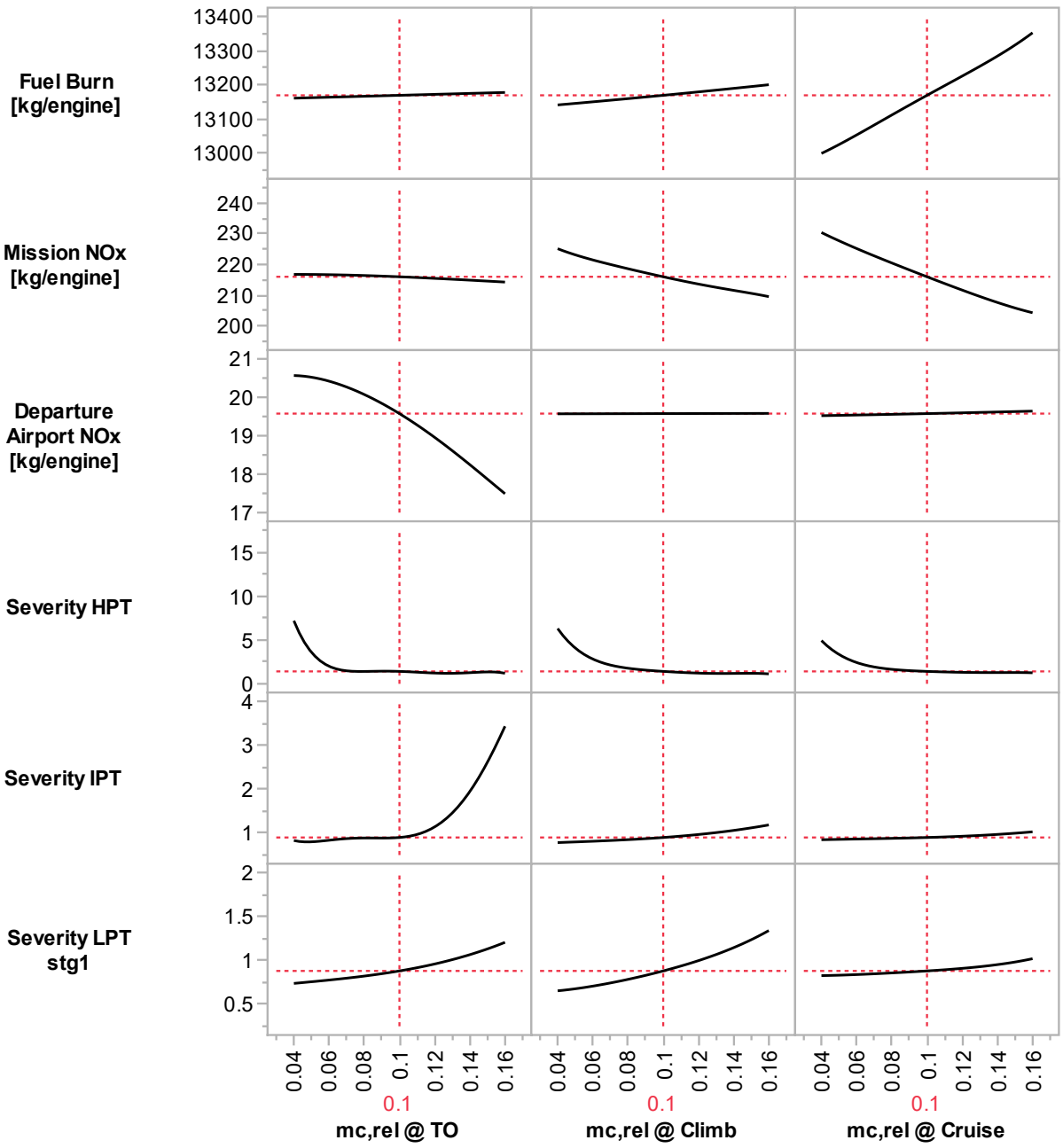

Fig. 14 Mapping the effect of cooling flow at take-off, climb and cruise on a 1480nmi mission (fuel burn, NOx, HPT severity, IPT severity, LPT stg1 severity)

D. Effects of severity factors in engine's life

The severity factors presented above define the ratio of damage to components with respect to a reference mission. To understand how this factor affects the overall life of the engine, the severity factor needs to be used in a model that can reflect the impact of cooling flow on the probability of failure of the engine. Weibull analysis is widely used to make predictions about the life of products in several sectors [28]. The Weibull distribution can be described by Eq. (9).

$$f(x|\eta,\beta) = \frac{\beta x^{\beta-1}}{\eta^{\beta}} e^{\left(\frac{-x}{\eta}\right)^{\beta}} \tag{9}$$

where η and β is the scale and shape parameters respectively. This parameterization of the Weibull distribution has the useful property that, for a constant c;

$$f(x|c\eta,\beta) = \frac{1}{c} f(cx|\eta,\beta) \tag{10}$$

such that increasing (decreasing) the scale parameter while holding the shape parameter constant is equivalent to stretching (compressing) the probability density function (pdf). This property provides a useful mechanism to model changes in the life of the engine components for different cooling flows by dividing the scale parameter by the severity factor. It is useful to calculate the probability of failure of the i'th component before a maintenance event at the time T_{maint}, denoted $P_{fail}^{(i)}(x \leq T_{maint})$, which can be calculated using the cumulative distribution function described by:

$$F(x|\eta,\beta) = 1 - e^{-\left(\frac{1}{\beta}\right)^{\eta}} \tag{11}$$

such that $P_{fail}^{(i)}(x \leq T_{maint}) = F(T_{maint}|\eta_i,\beta_i)$ where η_i and β_i are the scale and shape parameters of the i'th component respectively.

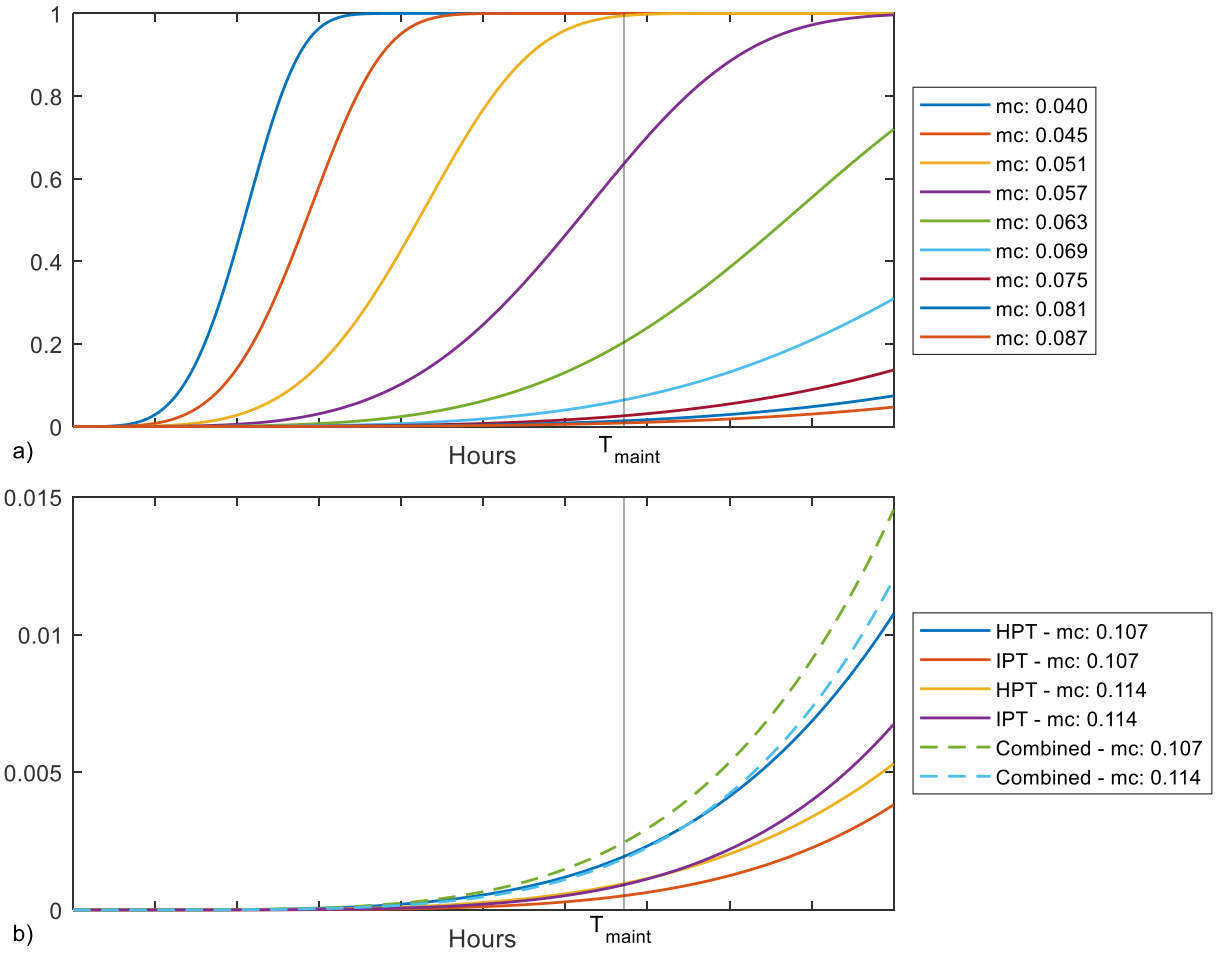

Fig. 15 a) Weibull cumulative distribution variation for different cooling flow values. Cooling flow can be used to reduce the probability of failure before a planned maintenance (blue vertical line) at the cost of the engine performance. b) Cumulative distribution of two engine components and combined distribution. Cooling flow has different effects on the engine's components depending of its location. The combination of these effects determines the probability of failure of the engine.

Varying the cooling flow setting has different effects on the engine's components depending on its location (Fig. 15). For instance, it can be seen that high cooling flow can extend the life of the HPT blade. This is in contrast to the IPT blade where the low cooling flow has a positive effect in terms of life. To analyze how changes in the cooling flow affect the probability of failure of an engine as a whole, the cumulative distribution function for the engine is constructed as

$$\bar{F}(x) = \prod_i 1 - F(x|\eta_i, \beta_i). \tag{12}$$

The probability of failure for the engine before a maintenance event is calculated multiple times at different levels of cooling. This analysis considers the current life of all the engine's components (requiring a small modification to $\bar{F}(x)$) and a cooling flow level. In this example, the cooling flow is only applied to HPT and IPT blades. Fig. 16 shows the probability of observing an unplanned failure before a predefined maintenance event and the fuel consumption for different cooling flows. As expected by the results in Fig. 13, the figure shows that the probability of failure increases for extreme (low and high) cooling flow levels.

Results such as that shown in Fig. 14 could be used to support engineers to make in-service control policy decisions. For example, when there is excess capacity available in a maintenance shop, decision-makers may be willing to risk higher failure rates in order to reduce fuel burn. Similarly, when there is limited capacity, it is more beneficial to minimize failure rates at the cost of higher fuel burn – and the minimum fuel burn that satisfies a failure rate criterion can be chosen.

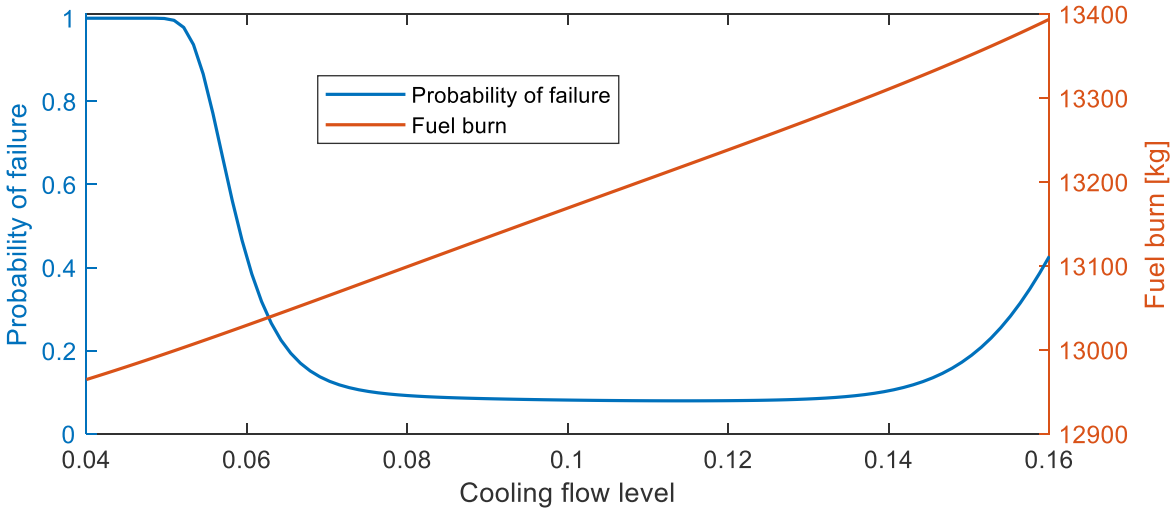

Fig. 16 Probability of unplanned failure before scheduled maintenance (blue line) and fuel consumption (orange line) for different levels of cooling flow

V. Conclusion

The effects of variable HPT blade cooling on hot gas path component life, emissions and fuel performance have been investigated. Despite the short take-off duration, the relative cooling flow selection at take-off has a huge impact on HPT, IPT and LPT stg1 severity, while the increase in the instantaneous fuel consumption becomes negligible due to the short duration of this phase. Increased HPT blade cooling protects the HPT blade, but the increase in TET to achieve the same target thrust has a negative impact on the life of the downstream hot gas path components which are usually non-cooled (IPT and LPT), and are directly exposed to the higher gas temperatures. Cruise is operated at lower temperature ranges and rotational speeds so any impact it has on component life is mainly driven by the long duration. However, cruise consumes a significant fraction of the total mission fuel, especially in long-range aircraft, so the selection of a lower cooling bleed at cruise can offer a considerable reduction in fuel consumption. Compared to take-off and cruise, climb conditions are in-between, in terms of duration, temperature and range. There is a more balanced sensitivity between fuel and HPT blade life with variable climb cooling, and a trade-off may be relevant based on an economic scenario.

Based on the mapping of variable cooling flow effects in this paper, a cooling schedule can be selected as a response to various scenarios and economic conditions. At standard conditions, it may be reasonable to select high cooling at take-off to prolong HPT life, while a reduction in cooling at cruise may offer significant savings in fuel burn and fuel cost. However, under special conditions and specific scenarios, the best option might not be the aforementioned. Some interesting scenarios include:

- The operational severity of a specific component may be decided to be reduced and prolong its life when spare parts for this component are temporarily unavailable.
- The overall engine severity or the severity of the component which is getting closer to replacement or restoration time may be reduced to prolong TOW at the expense of higher fuel consumption because there are no spare engines and an engine removal would cause longer aircraft grounding which can disrupt operations, especially during peak travel seasons.
- On the other side, if there is no specific need to further prolong TOW, if the time for a planned HPT-related shop visit is approaching, fuel savings can be increased by increasing the severity of the HPT with reduced cooling, as long as it doesn't exceed an acceptable limit of failure probability.
- When the engine is degraded and the operating temperatures are increased, manipulating the cooling flow can contribute towards satisfying airport NOx emissions.
- A sudden increase in fuel price may modify the optimum economic trade-off between engine severity (which can be related to maintenance reserves) and fuel consumption. On the other side, a drop in fuel price may swift the optimum towards protecting HPT life with increased fuel consumption.

Furthermore, it was observed that the variable cooling alters EGT by up to 50K at take-off for clean engine condition, before considering any degradation, This EGT variation may have implications for the current diagnostic and health-monitoring practices. The EGT redline may need to be considered variable as a function of the variable cooling flow setting.

Considerations for the decision-making about cooling flow policies and schedules were discussed qualitatively to understand the trade-off and opportunities. In future work, the surrogate functions for mapping the variable cooling flow effects will be applied to the optimization scenarios discussed above quantitatively. Furthermore, more variable engine parameters can be mapped and combined with the variable cooling flow using the presented methods. Finally, the effects of variable cooling on life should be investigated for more damage mechanisms, such as hot corrosion and thermomechanical fatigue.

Appendix

Table 1 Engine performance model design point

BPR	6.4
Fan PR	1.48
IPC PR	7.475
HPC PR	3.56
Altitude	10668 m
Mach	0.84

Table 2 Engine geometry and properties for blade cooling model

Number of HPT rotor blades	80
Cooling channels per HPT blade	5
Cooling channel hydraulic diameter	0.004
TBC thickness	150 um
Blade wall thickness	0.002 m
TBC thermal conductivity	1.5 W/mK
Blade thermal conductivity	25.8 W/mK
HPT blade span	0.0745 m
IPT blade span	0.0931 m
LPT stg1 span	0.13 m

Table 3 Aircraft model

Wing Area	427.8 m^2
Wing Aspect Ratio	8.68
Tail Area	101.26 m^2
Tail Aspect Ratio	3.197
Fin Area	53.23
Fin Span	9.24 m^2
Fuselage Diameter	6.2 m
Fuselage Length	62.78 m
Nacelle Diameter	3.2 m
Nacelle Length	7.3 m

Acknowledgments

This research was funded by UK Research and Innovation (UKRI) under the project Powerplant Integration of Novel Engine Systems (PINES) with reference number 113263. For the purpose of open access, the authors have applied a Creative Commons Attribution (CC BY) license.

References

[1] Kim, S., Kim, D., Son, C., Kim, K., Kim, M., and Min, S. "A Full Engine Cycle Analysis of a Turbofan Engine for Optimum Scheduling of Variable Guide Vanes." *Aerospace Science and Technology*, Vol. 47, 2015, pp. 21–30. https://doi.org/10.1016/j.ast.2015.09.007.

[2] Kim, S. J., and Ki, T. "Variable Guide Vane Scheduling Method Based on the Kinematic Model and Dual Schedule Curves." *Applied Sciences (Switzerland)*, Vol. 10, No. 19, 2020, pp. 1–17. https://doi.org/10.3390/APP10196643.

[3] Przybylko, S. J. "Active-Control Technologies for Aircraft Engines." *33rd Joint Propulsion Conference and Exhibit*, 1997. https://doi.org/10.2514/6.1997-2769.

[4] James, W., and O'Dell, P. Derated Climb Performance in Large Civil Aircraft, Article 6. In *Boeing Performance and Flight Operations Engineering Conference*, 2005.

[5] Donaldson, R., Fischer, D., Gough, J., and Rysz, M. "Economic Impact of Derated Climb on Large Commercial Engines." *2007 Boeing Performance and Flight Operations Engineering Conference*, 2007, pp. 8.1-8.11.

[6] Lattime, S. B., and Steinetz, B. M. "Turbine Engine Clearance Control Systems: Current Practices and Future Directions." *38th AIAA/ASME/SAE/ASEE Joint Propulsion Conference and Exhibit*, No. September, 2002. https://doi.org/10.2514/6.2002-3790.

[7] Chapman, J. W., Kratz, J., Guo, T. H., and Litt, J. "Integrated Turbine Tip Clearance and Gas Turbine Engine Simulation." *52nd AIAA/SAE/ASEE Joint Propulsion Conference, 2016*, 2016, pp. 1–16. https://doi.org/10.2514/6.2016-5047.

[8] Xu, L., Bo, S., Hongde, Y., and Lei, W. Evolution of Rolls-Royce Air-Cooled Turbine Blades and Feature Analysis. No. 99, 2015, pp. 1482–1491.

[9] Special Metals Corporation. *Inconel 718*. 2007.

[10] Nowotnik, A. "Nickel-Based Superalloys." *Reference Module in Materials Science and Materials Engineering*, No. December 2016, 2016. https://doi.org/10.1016/b978-0-12-803581-8.02574-1.

[11] Gregory, B., and Moroz, O. Gas Turbine Cooling Review. Global Gas Turbine News, , 2015.

[12] Bunker, R. S. "Cooling Design Analysis." *Gas Turbine Handbook*, 2006, pp. 295–309.

[13] Horlock, J. H., Watson, D. T., and Jones, T. V. "Limitations of Gas Turbine Performance Imposed by Large Turbine Cooling Flows." *Journal of Engineering for Gas Turbines and Power*, Vol. 123, No. 3, 2001, pp. 487–494. https://doi.org/10.1115/1.1373398.

[14] Lallini, V., Janikovic, J., Pilidis, P., Singh, R., and Laskaridis, P. "A Calculation Tool of a Turbine Cooling Air Schedule for General Gas Turbine Simulation Algorithms." *Journal of Turbomachinery*, Vol. 134, No. 4, 2012, p. 041003. https://doi.org/10.1115/1.4003648.

[15] Torbidoni, L., and Massardo, A. F. "Analytical Blade Row Cooling Model for Innovative Gas Turbine Cycle Evaluations Supported by Semi-Empirical Air-Cooled Blade Data." *Journal of Engineering for Gas Turbines and Power*, Vol. 126, No. 3, 2004, p. 498. https://doi.org/10.1115/1.1707030.

[16] Giannakakis, P., Laskaridis, P., Nikolaidis, T., and Kalfas, A. I. “Toward a Scalable Propeller Performance Map.” *Journal of Propulsion and Power*, Vol. 31, No. 4, 2015, pp. 1073–1082. https://doi.org/10.2514/1.B35498.
[17] Laskaridis, P., Pilidis, P., and Kotsiopoulos, P. An Integrated Engine-Aircraft Performance Platform for Assessing New Technologies in Aeronautics. 2005.
[18] Apostolidis, A. *Turbine Cooling and Heat Transfer Modelling for Gas Turbine Performance Simulation*. Cranfield University, 2015.
[19] Eshati, S., Laskaridis, P., Haslam, A., and Pilidis, P. The Influence of Humidity on the Creep Life of a High Pressure Gas Turbine Blade: Part I Heat Transfer Model. No. 3, 2012, pp. 281–288.
[20] Schneider, W., Hammer, J., and Mughrabi, H. “Creep Deformation and Rupture Behaviour of the Monocrystalline Superalloy CMSX-4: A Comparison with the Alloy SRR 99.” *Superalloys*, 1992, pp. 589–598. https://doi.org/10.7449/1992/superalloys_1992_589_598.
[21] Fuchs, H. O., Stephens, R. I., and Saunders, H. *Metal Fatigue in Engineering*. 1981.
[22] Meier, S. M., Nissley, D. M., Sheffler, K. D., and Cruse, T. A. “Thermal Barrier Coating Life Prediction Model Development.” *Proceedings of the ASME Turbo Expo*, Vol. 5, No. Figure 1, 1991. https://doi.org/10.1115/91-GT-040.
[23] Abu, A. O., Eshati, S., Laskaridis, P., and Singh, R. “Aero-Engine Turbine Blade Life Assessment Using the Neu/Sehitoglu Damage Model.” *International Journal of Fatigue*, Vol. 61, 2014, pp. 160–169. https://doi.org/10.1016/j.ijfatigue.2013.11.015.
[24] Chandrasekaran, N., and Guha, A. “Study of Prediction Methods for NOx Emission from Turbofan Engines.” *Journal of Propulsion and Power*, Vol. 28, No. 1, 2012, pp. 170–180. https://doi.org/10.2514/1.B34245.
[25] International Civil Aviation Organization (ICAO). ICAO Aircraft Engine Emissions Databank. https://www.easa.europa.eu/en/domains/environment/icao-aircraft-engine-emissions-databank.
[26] SAS. JMP. https://www.jmp.com/en_us/home.html.
[27] ICAO. *ICAO Carbon Emissions Calculator Methodology - Version 10*. 2017.
[28] Life Data Analysis (Weibull Analysis). https://www.weibull.com/basics/lifedata.htm.